PROCEEDINGS, TOUGH Symposium 2006
Lawrence Berkeley National Laboratory, Berkeley, California, May 15–17, 2006

TOUGH AND THE BOUNDARY ELEMENT METHOD IN THE ESTIMATION OF THE NATURAL STATE OF GEOTHERMAL SUBMARINE SYSTEMS

Mario César Suárez Arriaga[1] and Fernando Samaniego V.[2]

[1] Faculty of Sciences, Michoacan University - UMSNH
[2] Faculty of Engineering, National University of Mexico- UNAM
Edificio B, Ciudad Universitaria
Morelia, Michoacan, 58090, Mexico
e-mail: msuarez@zeus.umich.mx

ABSTRACT

In this work we present a general updated description of geothermal submarine reservoirs and an evaluation of the amount of energy contained in these important natural systems. To estimate the natural state of these reservoirs we use the classical Boundary Element Method (BEM) and suggest a simple way to couple this technique to TOUGH2 through the INPUT file. Submarine geothermal reservoirs contain essentially an infinite amount of energy. The deep submarine heat is related to the existence of hydrothermal vents emerging in many places along the oceanic spreading centers between tectonic plates. These systems have a total length of about 65,000 km in the Earth's oceanic crust. The deep resources are located at certain places along the rifts between tectonic plates of the oceanic crust at more than 2000 m below sea level. Shallow resources are found near to continental platforms between 1 m and 50 m depth and are related to faults and fractures close to the coasts. Both types of resources exist in the Gulf of California, Mexico. To model these systems the initial mathematical problem is expressed in terms of boundary integral equations, fundamental solutions and boundary conditions of mixed type. The field main functions are pressure and temperature. The versatility and power of the BEM allows the efficient treatment of very complex or unknown reservoir geometry, without requiring discretization of the whole domain occupied by the system. This capability permits efficient testing of different boundary conditions to estimate several thermodynamic initial states at any desired interior point of the domain occupied by the reservoir under specific conditions. Unfortunately, the classical BEM is limited to single-phase flow in homogeneous media and cannot be fully applied to flow problems in heterogeneous systems. In this last case there is no fundamental solution. To overcome this difficulty after an initial state is estimated, TOUGH2 can be used to improve the initial simulation. The few available data on hydrothermal vents are very useful to estimate the amount of energy flowing from the ocean floor. In this way, it is possible to estimate initial conditions knowing only heat fluxes and temperatures at fissures and chimneys using this hybrid technique.

INTRODUCTION

Hydrothermal circulation at deep oceanic ridges is a fundamental complex process controlling mass and energy transfer from the interior of the Earth through the oceanic lithosphere, to the hydrosphere and to the atmosphere. Submarine hydrothermal interactions influence the composition of the oceanic crust and the oceans' chemistry. The fluid circulating in seafloor hydrothermal systems is chemically altered due to processes occurring during its passage through the oceanic crust at elevated temperatures and pressures. This mechanism produces hydrothermal vent fields that support diverse biological communities starting from microbial populations that link the transfer of the chemical energy of dissolved chemical species to the production of organic carbon, (Humphris *et al.*, 1995). The eventual transfer of some gases from the ocean to the atmosphere extends the influence of hydrothermal activity far beyond the oceans themselves. The understanding of these mass and energy flows among the complex geological, chemical, geophysical and biological subsystems requires the development of integrated models that include the interactions between them. Because of their complexity and of the scarcity of real data, the modeling and simulation of submarine reservoirs is cumbersome and uncertain. The BEM is a numerical technique for solving elliptic and convection-diffusion partial differential equations (PDE). The BEM relates boundary data and boundary integral equations to the internal points of the solution domain in a very effective and accurate way. This is a suitable method to quickly estimate several possible initial states of reservoirs when only a few data are available. In this paper we show the potential advantages of the BEM over other numerical methods and the way it can be coupled to TOUGH2. We also outline the fundamental characteristics of submarine hydrothermal systems and present a preliminary evaluation of their energy content.

TOUGH2 AND SUBMARINE RESERVOIRS

TOUGH2 is a powerful numerical code for solving PDE's and for simulating the coupled transport of water, energy, air, CO_2 and other components in porous/fractured media (Pruess *et al*., 1999). It solves

systems of non-linear PDE's of parabolic type. The general integral form of these equations is:

$$\frac{\partial}{\partial t}\int_{V_n}\rho_k\,dV+\int_{V_n}\vec{\nabla}\cdot\vec{F}_k\,dV=\int_{V_n}q_k\,dV \qquad (1)$$

Where V_n represents any porous medium flow domain, ρ_k is the density of some physical property (mass, energy), $\boldsymbol{F}_k$ is the flux of mass/energy and q_k is an injection/production term in V_n. The flux vector derives from the gradient of a field variable (pressure or temperature). The subindex k means that Eq. (1) holds for a multi-phase treatment of different components in the mass/energy balance equations, including convection and heat conduction in rock, water, air, gases, etc. For further details, please refer to the *TOUGH2 User's Guide (ibid.)*.

Equation (1) is numerically solved using the Integral Finite Difference Method (IFDM). This technique contains aspects of both major numerical methods, Finite Differences (FD) and Finite Elements (FE). These three methods require discretization of the whole solution domain Ω in the form: $\Omega=\sum_{n=1}^{N}V_n$.

The need to discretize the whole domain is the main reason for computation cost and of the total CPU time needed to solve a particular problem. In the potential application of TOUGH2 to submarine geothermal reservoirs, the first practical problems are the insufficiency of both available field data to simulate these systems and the total absence of production history.

THE BEM FOR ELLIPTIC PROBLEMS

During the numerical estimation of the initial state of a reservoir it is clear that, after a great number of time steps, the transient term in eq. (1) becomes practically zero. Thus for this problem, equation (1) becomes a PDE of elliptic type. The BEM is specifically indicated for linear elliptic PDE in homogeneous media. In this type of physical problems the BEM is clearly superior to FD, IFD and FE methods in both accuracy and efficiency. Mainly, because all these methods demand the discretization of the whole solution domain Ω. The key feature of the BEM is that only the surface of the porous medium needs to be discretized. The field variable can be calculated with high precision at any point in the interior of the domain using only the known values of the function at the boundary of Ω. The BEM provides an effective reduction of the dimension of the PDE solution space. As a result, improved numerical accuracy and lesser use of computational resources are obtained. Differential problems that can be solved on a Notebook using the BEM, could require a cluster or a workstation, or even a supercomputer using any of the other methods for the same level of accuracy and for the same degree of geometric complexity of the reservoir boundary (Cruse and Rizzo, 1975; Ameen, 2001; Pozrikidis, 2002). To illustrate the method, we solve an elliptic problem representing a stationary temperature (or pressure) distribution, described by the Poisson's equation with mixed boundary conditions (Figure 1):

$$\begin{aligned}&\Delta T=f(\vec{P}),\ \forall\ \vec{P}=(x,y)\in\Omega\subset\mathbb{R}^2,\\&T(\vec{P})=u_T(\vec{P}),\ \forall\ \vec{P}\in\Gamma_T,\\&\frac{\partial T}{\partial n}(\vec{P})=u_n(\vec{P}),\ \forall\ \vec{P}\in\Gamma_N\\&\partial\Omega=\Gamma=\Gamma_T\bigcup\Gamma_N\end{aligned} \qquad (2)$$

Let's assume first that $f = 0$ (Laplace PDE). Applying the Green's theorem and the fundamental solution to the integral form of eq. (2) (see Appendix) we obtain:

$$T(\vec{P})=-\frac{1}{2\pi}\int_{\Gamma}\left[Ln\left\|\vec{P}-\vec{q}\right\|\frac{\partial T(\vec{q})}{\partial n}-\frac{T(\vec{q})}{\left\|\vec{P}-\vec{q}\right\|}Cos\,\theta\right]ds$$

$$\forall\ \vec{P}\in\Omega,\ \vec{q}\in\partial\Omega,\ \theta=\measuredangle(\vec{r}_{Pq},\vec{n}),\ \vec{n}=normal\ to\ \Gamma\ at\ \vec{q} \qquad (3)$$

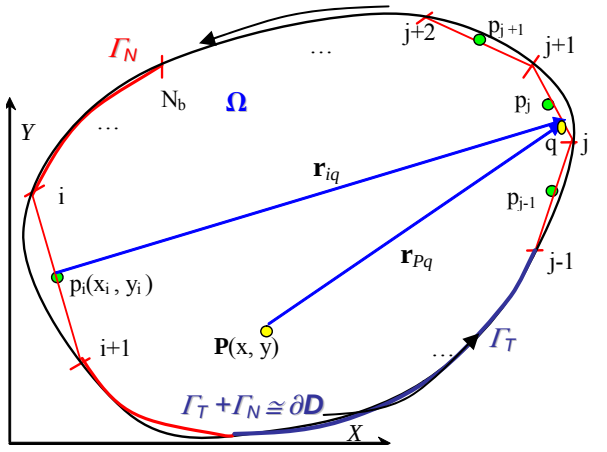

Figure. 1. Discretization of the boundary of Ω in the 2D solution domain of the PDE (2).

The boundary $\partial\Omega$ is discretized into Γ_j (j =1, N_b) boundary elements which can be linear, parabolic, cubic splines in 2D. In the 3D case, the boundary elements can be triangles, rectangles, arcs, etc.

BEM Solution of the Poisson Equation

Let us assume now that $f \neq 0$ (Poisson PDE), applying the same methodology proposed by Katsikadelis (2002) we obtain:

$$\forall\ \vec{P},\vec{Q}\in\Omega:\ T(\vec{P})=\int_{\Omega} v(\vec{P},\vec{Q})\, f(\vec{P})\, d\Omega$$
$$-\int_{\Gamma}\left[v(\vec{P},\vec{q})\frac{\partial T(\vec{q})}{\partial n}-T(\vec{q})\frac{\partial v}{\partial n}(\vec{P},\vec{q})\right] d\,s \qquad (4)$$
$$\textit{Where}\ \ \vec{q}\in\Gamma\ \textit{and}\ v(\vec{P},\vec{q})=\frac{Ln\left(\left\|\vec{P}-\vec{q}\right\|\right)}{2\pi}$$

The auxiliary function v is the Fundamental Solution of the Singular form of Laplace Equation (Appendix) and plays a crucial role in the classical BEM. For time-dependent problems of parabolic type the BEM can also be applied using two subsidiary techniques:

a) Solving first the PDE in time using FD, then applying the BEM to the time-discretized equations.
b) Removing the time dependence of the PDE using the Laplace Transform.

The BEM Numerical Implementation: an example

Let us assume that each Γ_j is a constant linear segment. The discretization of the boundary Γ (Fig. 1) in Eq. (3) implies that:

$$\Gamma_T \bigcup \Gamma_N = \Gamma \approx \bigcup_{j=1}^{N_b} \Gamma_j \qquad (5)$$

Consequently Eq. (3) can be discretized as:

$$\frac{T^i}{2}=-\sum_{j=1}^{N_b}\int_{\Gamma_j} v(\vec{p}_i,\vec{q})\frac{\partial T(\vec{q})}{\partial n_j}ds\ + \\ +\sum_{j=1}^{N_b}\int_{\Gamma_j} T(\vec{q})\frac{\partial v(\vec{p}_i,\vec{q})}{\partial n_j} \qquad (6)$$

or equivalently as:

$$\sum_{j=1}^{N_b} H_{ij}\, T^j=\sum_{j=1}^{N_b} G_{ij}\ \frac{\partial T}{\partial n}^j \qquad (7)$$

The influence coefficients H_{ij} and G_{ij} are integral forms equal to:

$$H_{ij}=\int_{\Gamma_j}\left(\frac{\partial v}{\partial n_j}ds\right)-\frac{\delta_{ij}}{2};\ G_{ij}=\int_{\Gamma_j} v(\vec{p}_i,\vec{q})\,ds \qquad (8)$$

From Eq. (7) we finally obtain the linear system:

$$\mathbf{H}\cdot\vec{T}\ =\ \mathbf{G}\cdot\vec{T}_n$$
$$T^j=(u^j);\ T_n{}^j=\frac{\partial T^j}{\partial n}=(u_n{}^j) \qquad (9)$$

Because of the assumed mixed boundary conditions, u_T in Γ_T and u_n in Γ_N, there are unknown quantities in both sides of Eq. (9). Consequently we need to separate the identified u's from the not known u's in order to obtain a consistent system of linear equations. As an example, the system for $N_b = 4$ is:

$$\begin{pmatrix} H_{11} & H_{12} & H_{13} & H_{14}\\ H_{21} & H_{22} & H_{23} & H_{24}\\ H_{31} & H_{32} & H_{33} & H_{34}\\ H_{41} & H_{42} & H_{43} & H_{44}\end{pmatrix}\bullet\begin{pmatrix} u^1\\ u^2\\ T^3\\ T^4\end{pmatrix}= \\ \begin{pmatrix} G_{11} & G_{12} & G_{13} & G_{14}\\ G_{21} & G_{22} & G_{23} & G_{24}\\ G_{31} & G_{32} & G_{33} & G_{34}\\ G_{41} & G_{42} & G_{43} & G_{44}\end{pmatrix}\bullet\begin{pmatrix} T_n{}^1\\ T_n{}^2\\ u_n{}^3\\ u_n{}^4\end{pmatrix} \qquad (10)$$

Let us suppose that the u^j are the known quantities and the T^j are the unknown variables. Moving all the unknowns to the left hand side of equation (10) we obtain the final linear system:

$$\mathbf{A}\cdot\vec{\mathbf{T}}=\mathbf{B}\qquad\Leftrightarrow$$
$$\begin{pmatrix} -H_{13} & -H_{14} & G_{11} & G_{12}\\ -H_{23} & -H_{24} & G_{21} & G_{22}\\ -H_{33} & -H_{34} & G_{31} & G_{32}\\ -H_{43} & -H_{44} & G_{41} & G_{42}\end{pmatrix}\cdot\begin{pmatrix} T^3\\ T^4\\ T_n{}^1\\ T_n{}^2\end{pmatrix}=\cdot\begin{pmatrix} B^1\\ B^2\\ B^3\\ B^4\end{pmatrix} \qquad (11)$$
$$B^i=H_{i1}u^1+H_{i2}u^2-G_{i3}u_n{}^3-G_{i4}u_n{}^4$$

The matrix in this system is full and non symmetric, but is at least four times smaller than the equivalent matrix obtained from FD, FE or IFD. This result can be easily generalized for any $N_b > 4$. We are ready to apply the BEM to submarine reservoirs.

SUBMARINE GEOTHERMAL SYSTEMS

Geothermal Discharges, Plumes and Venting

Most of the known vents are at the mid-ocean ridge systems (MORS) in the deep sea (Damm, 1995). Magmatic processes provide the energy to drive hydrothermal circulation of seawater through the oceanic crust causing rock-seawater interaction at temperatures between 200°C and 400°C, (Suárez & Samaniego, 2005). The resulting mechanism gives rise to venting at seafloor depth, ranging between 840 and 3600 meters depth (Fig. 2) and contributing considerably to the global balance of the total Earth's heat (Fornari and Embley, 1995). This venting is associated with fissures located directly above magma injection zones.

The observed vent fields are tens of meters in diameter ranging in area between 4 – 800 m^2 ,

(Humphris *et al.*, 1995). The heat input from those systems affects the mid-depth circulation of the oceans. Hydrothermal plumes are created by the thermal and chemical fluid input from submarine hot spring systems into the deep sea (Figs. 2 and 3).

Figure 2. The birth of a plume at the top of a submarine chimney located 3000 m depth in the Pacific Ocean (BP-BBC, 2004).

The vents in the deep sea are markedly short-lived and ever changing. The depth and size of the heat source and the type of permeability related to faults and fractures acting as recharge conduits, will determine the longevity of a vent area (Fornari and Embley, 1995). The plumes hold many clues to the characteristics of hydro-thermal venting and its effect on the ocean. The rising plumes entrain deeper and saltier water, carrying it up in the water column affecting the thermoaline circulation of the oceans (Damm, 1995). The plumes' active discharge orifices cover only a minuscule percentage of the seafloor. But there is an enormous range of temporal and spatial scales involved in these events. Baker *et al.* (1995) found that the hydrothermal fluids discharged from vents form plumes that are rapidly diluted in the seawater and the mixture rises hundreds of meters and spreads laterally from tens to thousands of kilometers. Those plumes formed by mixing of seafloor vent fluids and ambient seawater are easily detectable by physical and chemical tracers. That is why the careful study of plumes is a useful tool for hydrothermal exploration.

Black and White Smoker Chimneys

Divergent plate movements in the deep sea produce fissures, allowing vertical transfer of magmatic heat toward the ocean floor. As cold seawater enters those fissures, it becomes hot and is chemically changed during its contact with the rock. In this way the oceanic crust is cooled significantly by convection. The recharge areas where seawater enters the crust are diffuse and widespread (Humphris *et al*, 1995). At seafloor hydrothermal vent sites, hot, acidic hydrothermal fluids are injected into cold, alkaline seawater, resulting in precipitation of vent deposits and particle-rich plumes (Kingston, 1995). These deposits and plumes are the surface expression of large hydrothermal systems that transfer significant heat and mass from the mantle and crust to the hydrosphere. Many vent fields have vertical structures forming chimneys built of materials which precipitate from the heated vent fluid as it mixes with seawater. Black smoker chimney walls are initially emplaced as hydrothermal fluid mixes turbulently with seawater (Fig. 3). This occurs because of "… *the subsequent dominance of horizontal transport across the wall, mineral dissolution and precipitation within pore spaces of the wall, and deposition of Cu-Fe sulfide along the inside of the flow conduit*", (*ibid*).

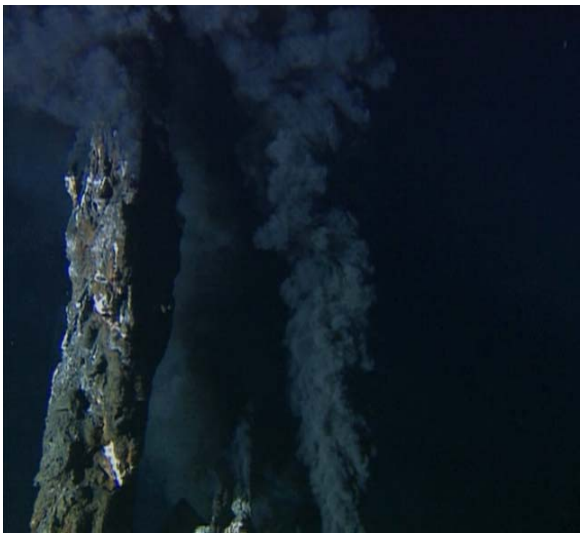

Figure 3. Two natural chimneys in the Pacific Ocean, discharging fluids at temperatures of about 350°C (BP-BBC, 2004).

During dives with the submarine Alvin at the Gulf of California (Mercado, 1990) diverse hydrothermal manifestations were observed. The *Hanging Gardens* were discovered at 2600 m depth (Fig. 4) and similar impressive natural chimneys up to 6 m high were also observed (Fig. 3). Those almost metallic natural chimneys are formed in part by iron and copper sulfides and discharge spouts of water at 350°C. Mercado (1990) reported sampling of sea water containing anomalies of methane, helium and hydrogen associated with geothermal fluids. The flow of hot water expelled by the chimneys, had an approximate speed of 250 cm/s flowing through diameters between 10 and 20 cm.

Figure 4. A strange "flower" or tube-worm opening in a submarine garden, (BP-BBC, 2004).

Kingston (1995) mentioned that initial models separate the formation of chimneys into stages. The first stage is precipitation of porous anhydrite walls that contain fine inclusions of sulfide. This stage occurs when hydrothermal fluid at 350°C exits the seafloor at velocities of about 100 cm/s and mixes with seawater at 2°C. Velocities measured in the hydrothermal plumes 3 to 5 cm above the orifices of chimneys at 21°N EPR varied from 70 to 236 cm/s (Kingston, 1995). The images shown in Figures 2 and 3 correspond to portions of plumes from black smokers with a heat flux of about 60 MW_T (thermal mega-Watts), venting into an ocean with a constant density gradient given by the following equation (Lupton, 1995):

$$N^2 = -\frac{g}{\rho_0}\frac{d\rho}{dz} = 1.5\times10^{-6}\ s^{-2} \qquad (12)$$

Where g is the gravity acceleration, ρ_0 is the average local density and $d\rho/dz$ is the vertical density gradient $d\rho/dz \approx 1.53\times10^{-4}$ kg/m^4. N is called the Brunt - Väisälä buoyancy frequency. Turner (1973; *op. cit. in* Humphris *et al*, 1995) established another useful equation to estimate the maximum height Z_M of rise of a plume as a function of the buoyancy flux F_0 and the frequency N:

$$Z_M = 5\left(\frac{F_0}{\pi}\right)^{\frac{1}{4}} N^{-\frac{3}{4}} \qquad (13)$$

From measured data reported by Lupton (1995), we obtain $F_0 = 0.17$ m^4 s^{-3}; using the frequency N, it is possible to estimate a maximum height for the plume: $Z_M \approx 370$ m above seafloor. After these models, a plume of 750 m height will correspond to a heat flux of about 1000 MW_T . Other measured thermal fluxes range from 1 to 93 MW_T , with an accepted average value for a single orifice of about 8 MW_T.

There is a weak dependence of Z_M on the effective heat flux. A megaplume observed at the Juan de Fuca ridge in 1986 was able to affect the water column up to 1000 m above the seafloor. Such a megaplume was the impressive result of an instantaneous and huge release of heat flux at the corresponding source. The fact that other megaplumes have been observed leads to the conclusion that the total convective heat outflowing from the ocean is discharged in the form of both continuous steady-state venting and megaplumes (Lupton, 1995).

Suárez and Samaniego (2005) reported an average heat flow in the Mexican Volcanic Belt of about 0.10 W_T/m^2. The submarine heat flow measured in some places of the Gulf of California was of the order of 0.34 W_T/m^2 at an average temperature of 330°C (Mercado, 1990). Using two models, Stein *et al*. (1995) predicted an average hydrothermal heat loss by conduction for the oceanic crust of about 1.5 W_T/m^2. The same parameter predicted for the ridges is between 2 and 100 MW_T/Km (per unit ridge length). The first value is for a slow ridge and the last value corresponds to a plume with a heat content of 1000 MW_T. Thus, the plumes remove more heat than the steady-state surface flux for the cooling lithosphere. Alt (1995) estimated that submarine hydrothermal discharges remove about 30% of the heat lost from oceanic crust.

Application of the BEM to Submarine Reservoirs, Temperature Distribution and Heat Flow

The PDE describing the natural state of a geothermal reservoir is approximately elliptic, because the transient changes are very slow. Eqs. (6-11) were programmed in a Fortran/90 code called BEMSub. We solved the line integrals of Eq. (8) by the Gauss-Legendre quadrature. We assumed a squared submarine reservoir of 1000 m × 1000 m in 2D.

Forty boundary elements were sufficient to estimate the temperature distribution in this reservoir using the BEM. The boundary conditions were zero heat flow at the lateral boundaries and constant but different temperatures at the bottom and top of the reservoir. To calculate the temperature we chosen 81 internal points uniformly distributed in the square. Although this number could be larger, 81 is enough to draw the surfaces and illustrate the results. We considered the numerical values shown in Table 1. The average thermal conductivity is 3.0 W/°C/m.

Table 1. Some Parameters of Submarine Reservoirs.

Field function	Minimum	Maximum
Pressure	190 bar	300 bar
Temperature	200 °C	700 °C
Fuid flow rate	70 cm/s	250 cm/s
Heat Flux	0.34 W_T/m^2	1.50 W_T/m^2

The idea of this application is simple: knowing the range of possible temperatures, what should be the fixed temperatures at the top and bottom of the reservoir able to reproduce the measured conductive heat flow? We considered two simulations, one for the heat flow measured in the Gulf of California (0.3 W_T/m^2) and a second one for the estimated average heat flux for the oceanic crust (1.5 W_T/m^2). The results are shown in Figures 5 and 6.

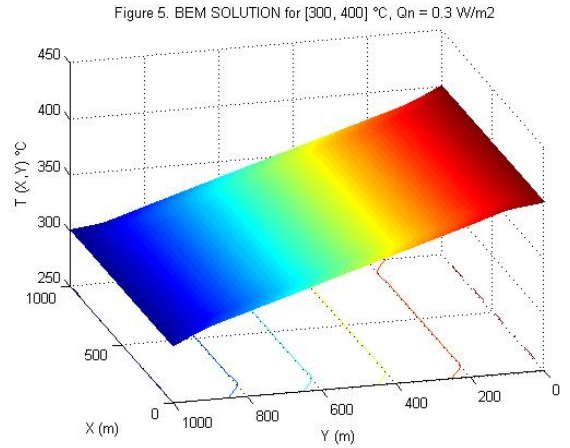

Figure 5. Temperatures fitting the flow of heat measured in the Gulf of California.

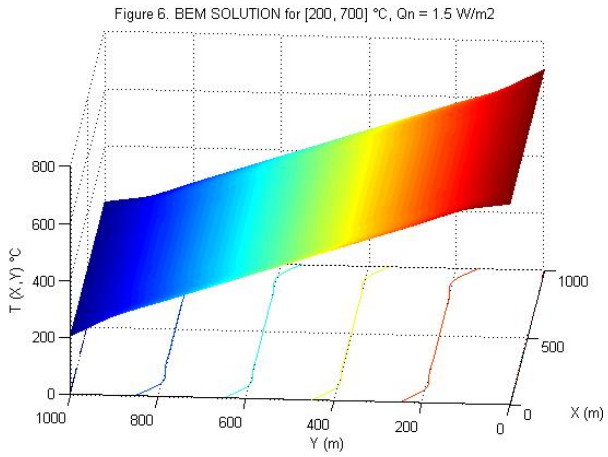

Figure 6. Temperatures fitting the average heat flow estimated for the entire oceanic crust.

Coupling the results of the BEM to TOUGH

Using the same data we prepared the INPUT deck of TOUGH for a regular mesh of 400 volumes of sizes 50 × 50 m each, for an EOS of pure water. The boundary conditions were the same, considering only the temperature initial state given by Figure 5. For the pressure we assumed a vertical linear distribution with the initial values at the top of the hypothetical submarine reservoir given in Table 2.

Table 2. Initial and final conditions at the Reservoir.

Field function	Top	Bottom
Pressure	190 bar	260 bar
Temperature	300 °C	400 °C
Fuid Density *	733.2 kg/m^3	189.4 kg/m^3
Heat Flow *	-0.29934 W_T/m^2	0.29934 W_T/m^2

The top of the reservoir is located 2600 m below sea level and the bottom is 1000 m deeper. After around 20 time steps, the temperature obtained with TOUGH is exactly the same as the distribution shown in Figure 5. The heat fluxes calculated with TOUGH at the top and bottom of the reservoir are of equal value but of opposite sign, indicating that a steady state was reached. This value is practically equal to that obtained with the BEM (0.3 W_T/m^2). The main difference is the calculation time. The BEM takes about 0.2 seconds of CPU time for a whole single calculation using a 3 GHz PC. TOUGH needs around 10^2 times more CPU time to achieve the same result. But if the starting thermodynamic point is far from these initial conditions for pressure and temperature, the total simulation time could be 10^5 times larger in the same computer, because of the need for small time steps.

CONCLUSIONS

- Deep submarine geothermal resources contain practically an infinite energy potential. Volcanic and tectonic processes control hydrothermal activity at mid-ocean ridge spreading centers, influencing all aspects of oceanography. The understanding of the mass and energy flows in these complex systems requires the development of integrated models that include the interactions among different subsystems.

- Using available data from different sources, we reported a preliminary estimation of the amount of convective and conductive energy contained in submarine systems escaping through fissures in the oceanic floor. Hydrothermal fluids at temperatures between 350°C and 400°C exits the chimneys on the seafloor at velocities of about 70 cm/s to 250 cm/s and mixes with deep seawater at 2°C. Measured thermal fluxes have an average value for

a single orifice of 8 MW_T. Some Mega-plumes of 750 m height correspond to heat fluxes of about 1000 MW_T.

- The main purpose of the simulation problem we have presented was to illustrate the easy and efficient use of the BEM in the estimation of the natural state of submarine reservoirs, knowing few parameters. The potential use of the BEM coupled to TOUGH could be enormously helpful in the computation of the initial state of any reservoir. This coupling could be also achieved in domain decompositions, using the extended BEM in subdomains that require detailed calculations and mesh refinement.

ACKNOWLEDGMENT

The authors are grateful to the National University of Mexico and to the Scientific Coordination (CIC) of the Michoacan University for their financial support.

REFERENCES

Alt, J., Subseafloor Processes in Mid - Ocean Ridge Hydrothermal Systems. *Geophysical Monograph* **91**, American Geophysical Union, 85-114, 1995.

Ameen, M. *Boundary Element Analysis: Theory and Programming*. Narosa Publishing House, 2001.

Archer, R. *Computing Flow and Pressure Transients in Heterogeneous Media using Boundary Element Methods*. Ph.D. Thesis. Department of Petroleum Engineering, Stanford University, CA, 2000.

Archer, R., Horne, R. and Onyejekwe, O. Petroleum Reservoir Engineering Applications of the Dual Reciprocity Boundary Element Method and the Green Element Method. 21st World Conference on the BEM. Oxford University, 1999.

Baker, E., C. German and H. Elderfield. Hydrothermal Plumes over Spreading-Center Axes: Global Distributions and Geological Inferences. *Geophysical Monograph* **91**, American Geophysical Union, 47-71, 1995.

Blue Planet: A Natural History of the Oceans. The Abyss. BBC/DVD No. 1. Eds. Folio and Tycoon Entertainment Group, 2004.

Cruse, T. and F. Rizzo. Boundary Integral Equation Method: Computational Applications in Applied Mechanics, 1995. *Applied Mechanics Conf. AMD*-Vol. 11, The Applied Mechanics Division, ASME. Rensselaer Polytechnic Institute, New York, 1975.

Damm, K. (1995), Controls on the Chemistry and Temporal Variability of Seafloor Hydrothermal Fluids. *Geophysical Monograph* **91**, American Geophysical Union, 222-247.

Fornari, D. and Embley, R. (1995), Tectonic and Volcanic Controls on Hydrothermal Processes at the Mid-Ocean Ridge: An Overview Based on Near-Bottom and Submersible Studies. *Geophysical Monograph* **91**, American Geophysical Union, 1- 46.

Humphris, S., R. Zierenberg, L. Mullineaux and R. Thomson, Editors. *Seafloor Hydrothermal Systems. Physical, Chemical, Biological and Geological Interactions*. *Geophysical Mono.* **91**, American Geoph. Union, ISBN 0-87590-048-8, 466 pp, 1995.

Katsikadelis, J. T. *Boundary Elements: Theory and Applications*. Elsevier, 2002.

Kingston, M. Modeling Chimney Growth and Associated Fluid Flow at Seafloor Hydrothermal Vent Sites. *Geophysical Monograph* **91**, American Geophysical Union, 158-177, 1995.

Lupton, J. Hydrothermal Plumes: Near and Far Field. *Geophysical Monograph* **91**, American Geophysical Union, 317-346, 1995.

Mercado, S. Manifestaciones Hidrotermales Marinas de Alta Temperatura (350 °C) Localizadas a 21°N, a 2600 m de Profundidad en la Elevación Este del Pacífico. *GEOTERMIA,* **6**, No. 3, 225-263, 1990.

Pita, R., C. *Cálculo Vectorial*. Prentice-Hall Hispano-americana, S.A., México, 1995.

Pozrikidis, C. *Boundary Element Methods*. Chapman & Hall / CRC Press, Boca Raton, FL, 2002.

Pruess, K., C. Oldenburg, and G. Moridis, *TOUGH2 User's Guide, Version 2.0*, Report LBNL-43134, Lawrence Berkeley National Laboratory, Berkeley, Calif., 1999.

Sato, K. *Accelerated Perturbation Boundary Element Model for Flow Problems in Heterogeneous Reservoirs*. Ph.D. Thesis. Department of Petroleum Engineering, Stanford University, CA, 1992.

Stein, C., S. Stein and A. Pelayo, Heat Flow and Hydrothermal Circulation. *Geophysical Monograph* **91**, American Geophysical Union, 425-445, 1995.

Suárez, A. M. and F. Samaniego. A Preliminary Evaluation of the Convective Energy Escaping from Submarine Hydrothermal Chimneys. *Proceedings, 30th Workshop on Geothermal Reservoir Engineering* Stanford University, CA, SGP-TR-176, 2005.

MATHEMATICAL APPENDIX

Stoke's and Green's Theorems

The main fundamental theorem supporting the BEM is the general Stoke's Theorem (Pita, 1995):

$$\int_\Omega d\omega = \int_\Gamma \omega,\ \Gamma = \partial\Omega,\ \Omega \subset \mathbb{R}^n,\ \Gamma \subset \mathbb{R}^{n-1} \qquad n = 1,2,3;\ \Gamma = \partial\Omega \text{ is the boundary of } \Omega \tag{14}$$

Where Ω is an open subset of $\mathbb{R}^n$, ω is any differential form defined in Ω. This simple and elegant theorem has many significant consequences. Let's define $\omega(x,y) = f(x,y) + g(x,y)$; Stoke's Theorem implies that:

$$\int_\Omega \left(\frac{\partial f}{\partial x} + \frac{\partial g}{\partial y} \right) dx\, dy = \int_\Gamma (f\, dy - g\, dx) \tag{15}$$

Assuming that (f, g) are the components of a gradient and defining a vector ***n*** normal to the curve Γ:

$$\vec{\nabla} F = \left(\frac{\partial F}{\partial x}, \frac{\partial F}{\partial y} \right) = (f, g);\ \vec{n} = (n_x, n_y) \Rightarrow$$

$$\int_\Omega (\Delta F)\, dx\, dy = \int_\Gamma \vec{\nabla} F \cdot \vec{n}\, ds = \int_\Gamma \frac{\partial F}{\partial n} ds \tag{16}$$

$$\text{Where: } \Delta F = \vec{\nabla} \cdot \left(\vec{\nabla} F \right) = \left(\frac{\partial^2 F}{\partial x^2} + \frac{\partial^2 F}{\partial y^2} \right)$$

This result implies the first form of Green's theorem:

$$f = u \frac{\partial v}{\partial x},\ g = v \frac{\partial u}{\partial y},\ u, v : \Omega \to \mathbb{R},\ u, v \in C^2_\Omega$$

$$\int_\Omega \left(u\, \Delta v + \vec{\nabla} u \cdot \vec{\nabla} v \right) dx\, dy = \int_{\partial\Omega} u \frac{\partial v}{\partial n} d\, s \tag{17}$$

Interchanging the roles of *u* an *v* in this formula and subtracting both results we finally arrive to the full expression of the general Green's Theorem:

$$\int_\Omega (u\, \Delta v - v\, \Delta u)\, d\Omega = \int_{\partial\Omega} \left(u \frac{\partial v}{\partial n} - v \frac{\partial u}{\partial n} \right) d\, s \tag{18}$$

$$\Omega \subset \mathbb{R}^n \text{ and } \partial\Omega \subset \mathbb{R}^{n-1},\ n = 1,2,3$$

The Distribution of Dirac (a *generalized function*)

Another fundamental result that supports the theory of the BEM concerns the Dirac's Delta distribution (Pozrikidis, 2002; Katsikadelis, 2002). It can be defined in 1, 2 or 3 dimensions and interpreted as a forced Laplace's equation for a field produced around a singular point. Let $\vec{P}$ *and* $\vec{P_0} \in \mathbb{R}^n$, be two points in the n-dimensional space (n = 1, 2, 3), where $\vec{P_0}$ is the location of a fixed singular point, $\vec{P}$ is any variable point of the field. The distribution of Dirac $\delta_n(\vec{P} - \vec{P_0})$ is a generalized function such that:

$$\delta_n(\vec{P} - \vec{P}_0) = \lim_{\beta \to \infty} \frac{\beta}{\pi} \exp\left(-\beta \,\| \vec{P} - \vec{P}_0 \|^2 \right)$$

$$\| \vec{P} - \vec{P}_0 \| = \sqrt{\sum_{k=1}^{n} (x_k - x_{0k})^2} \quad \text{for } n = 1,2,3 \tag{19}$$

Where β is a real positive parameter related to an arbitrary length. The following properties are easily demonstrated:

$$\begin{aligned}
&1)\ \delta_2(\vec{P} - \vec{P}_0) = \delta_1(x - x_0)\, \delta_1(y - y_0) \\
&2)\ \delta_3(\vec{P} - \vec{P}_0) = \delta_1(x - x_0)\, \delta_1(y - y_0)\, \delta_1(z - z_0) \\
&3)\ \delta_n(\vec{P} - \vec{P}_0) = 0 \ \ \forall\ \vec{P} \neq \vec{P}_0 \\
&4)\ \delta_n(\vec{P} - \vec{P}_0) = \infty \ \ \text{if } \vec{P} = \vec{P}_0 \\
&5)\ \int_\Omega \delta_n(\vec{P} - \vec{P}_0)\, d\Omega = 1 \ \ \forall\ \Omega \ni \vec{P}_0 \\
&6)\ \int_\Omega \delta_n(\vec{P} - \vec{P}_0)\, f(\vec{P})\, d\Omega = f(\vec{P}_0) \ \ \forall\ \Omega \ni \vec{P}_0
\end{aligned} \tag{20}$$

This last property establishes that the integral of the product of δ_n and an arbitrary function over a domain Ω containing the singular point $\vec{P_0}$ is equal to $f(\vec{P}_0)$, the value of the function at the singular point. Thus, if Ω does not contain $\vec{P_0}$ this integral is equal to zero.

The Fundamental Solution in the Free Space

Let $\vec{P}$ be any point, and $\vec{P_0}$ a heat point source located somewhere in the plane $\mathbb{R}^2$. The influence of the heat source is described by the Dirac's Delta distribution (see Appendix): $f(\vec{P}) = \delta(\vec{P} - \vec{P_0})$. The temperature field is described by the fundamental PDE (Pozrikidis, 2002) in polar coordinates:

$$\Delta T = \frac{d^2 T}{d r^2} + \frac{1}{r} \frac{d T}{d r} = \delta(\vec{P} - \vec{P}_0),$$

$$r = \left\| \vec{P} - \vec{P}_0 \right\| = \sqrt{(x - x_0)^2 + (y - y_0)^2} \tag{21}$$

The solution of this PDE plays a very important role in the BEM and is called the Singular or Fundamental Solution or the Free Space Function of Green. Its expression is:

$$v(\vec{P} - \vec{P}_0) = \frac{Ln(r)}{2\pi} \tag{22}$$

Applying these results to the PDE (2) with $f = 0$ we obtain:

$$\int_{\Omega}\left(T\,\Delta v - v\,\Delta T\right)d\,\Omega = \int_{\Omega}\left(0 - T(\vec{P}_0)\,\delta(\vec{P}-\vec{P}_0)\right)d\,\Omega \;\Rightarrow$$

$$T(\vec{P}) = \int_{\substack{\partial\Omega=\Gamma= \\ \Gamma_T+\Gamma_N}}\left(T(\vec{q})\frac{\partial v(\vec{q},\vec{P})}{\partial n} - v(\vec{q},\vec{P})\frac{\partial T(\vec{q})}{\partial n}\right)d\,s$$

$$\forall\ \vec{P},\vec{P}_0 \in \Omega \subset \mathbb{R}^n \ \textit{and}\ \vec{q} \in \partial\Omega \subset \mathbb{R}^{n-1}\ ,\ \ n = 1,2,3$$

(23)

This is the main solution of the classical BEM. The method has been extended to more complex problems, including transient PDE of parabolic type in heterogeneous media (Archer, 2000; Archer *et al.*, 1999; Sato, 1992).